ACS Macro Letters

Letter

pubs.acs.org/macroletters

Jamming of Knots along a Tensioned Chain

Vivek Narsimhan,[‡] C. Benjamin Renner,[†,‡] and Patrick S. Doyle*

Department of Chemical Engineering, Massachusetts Institute of Technology, Cambridge, Massachusetts 02139, United States

Supporting Information

ABSTRACT: We examine the motion of a knot along a tensioned chain whose backbone is corrugated due to excluded volume effects. At low applied tensions, the knot traverses the chain diffusively, while at higher tensions the knot makes slow, discrete hops that can be described as a Poisson process. In this "jammed" regime, the knot's long-time diffusivity decreases exponentially with increasing tension. We quantify how these measurements are altered by chain rigidity and the corrugation of the polymer backbone. We also characterize the energy barrier of the reptation moves that gives rise to the knot's motion. For the simple knot types examined thus far (3_1, 4_1, 5_1, 5_2), the dominant contribution to the energy landscape appears in the first step of reptation—i.e., polymer entering the knotted core. We hope this study gives insight into what physics contributes to the internal friction of highly jammed knots.

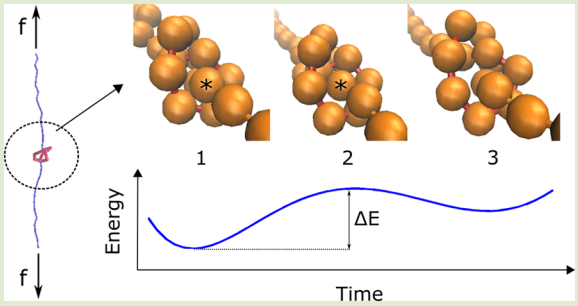

Ever since the discovery of knots in DNA,[1−3] there has been immense interest in understanding how these structures affect the mechanical and dynamical properties of these molecules.[4] A knot is defined as a self-entanglement that cannot be undone when the polymer chain is closed.[5] The topology of a knot is well-defined as long as it is far from the ends of a polymer chain, and the topology can be determined by closing the chain and then computing Alexander polynomials.[6] Experimentally, knots have been tied onto DNA[7] and actin[8] filaments via optical traps, and chemical synthesis techniques have been developed to create knotted loops up to five crossings.[9] Recently, researchers have also determined facile methods to create knotted DNA via an electric field,[10,11] and this work has led to microfluidic experiments examining how the coil−stretch transition is affected by the presence of knots.[12]

In some sense, knots are unavoidable for very long polymeric chains, as it has been proven that the knotting probability approaches unity as the chain size gets very large.[13,14] Indeed, knots have been found in capsid DNA,[1] proteins,[15−17] and other biological systems.[4] Bao et al. discovered that knots can self-reptate along a polymer contour due to thermal fluctuations.[7] This discovery has led several computational studies to quantify the knot's motion along a chain, whether it be convection due to a directed force[18−20] or diffusion under uniform tension.[21−23] In most of these studies, the tension on the polymer is comparable to or smaller than the Brownian forces—i.e., $f \sim O(kT/l_p)$ or smaller, where kT is the thermal energy and l_p is the persistence length of the chain. However, it is known that at large tensions knots can dynamically arrest—this has been observed for knots jamming during translocation through a nanopore.[24−27] Huang and Makarov briefly study jamming in their simulations,[23] positing that the knot's arrest is caused by the "bumpiness of the energy landscape of the knot created by intrachain interactions". We explore this topic in this Letter. We note that this area of research is of interest to the polymer physics community as it can provide insight into what effects contribute to the strong friction between chain entanglements.

We model our polymer as a bead−rod chain with hard-sphere interactions between nonconnected beads and bending interactions between adjacent rods. We tie a knot into the middle of the chain, apply a tension f at the ends, and track the knot's motion along the contour as a function of time (Figure 1a). There are three important length scales in this problem: l is the rod length, b is the bead diameter, and l_p is the persistence length of the chain. We will examine the effect of b and l_p on the dynamics of knot jamming. We anticipate that the excluded volume effects will become important as the chain segments in the knot are driven toward each other. In the parlance of Makarov and co-workers,[23,28] the bead size b sets the corrugation of the energy landscape along the polymer backbone. We note that this energy landscape is simpler than the one along a real polymer chain. However, recent experiments suggest that polymers like actin are corrugated at the monomer length scale,[29] which suggests that our idealized models may capture the essential physics giving rise to friction. We also note that several computational studies have observed jamming using soft bead−bead chains (i.e., $b = l$), which indicates that there is a clear interest in understanding knot jamming via these simple physical models.[23,24,27]

The details of the Brownian dynamics simulations are listed in the Supporting Information (SI). We let the polymer chain be much larger than the jammed knot size ($N \approx 100-300$

Received: October 15, 2015
Accepted: December 29, 2015

DOI: 10.1021/acsmacrolett.5b00737
ACS Macro Lett. 2016, 5, 123−127

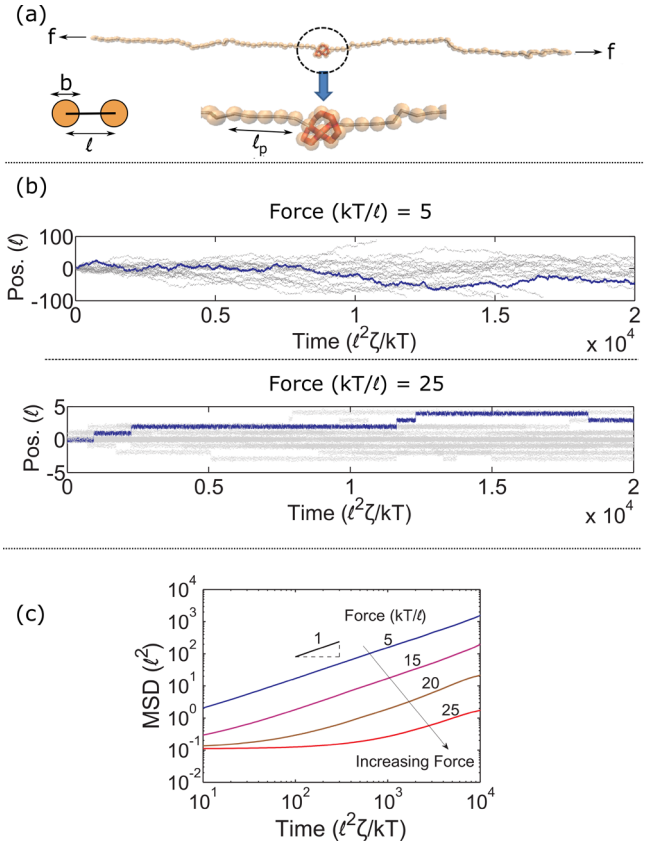

Figure 1. (a) Schematic of simulation. (b) Trajectories of a 3_1 knot for two different applied tensions. Highlighted curve is a trace from one run. (c) Mean-squared displacement of a 3_1 knot. For (b) and (c), the chain is flexible ($l = 2l_p$), and the bead size is equal to the rod distance ($b = l$).

compared to $N_k \approx 10-20$ beads) so that the knot's motion is insensitive to the polymer length and end effects (see SI). Like in other studies,[23] we neglect hydrodynamic interactions between chain segments and set the drag coefficient on each bead to be ζ. The length and time scales in which we report our results will be in terms of the rod length l and the diffusion time $l^2\zeta/kT$. To enforce the excluded volume interactions between the beads, we apply a stiff, harmonic potential between them when they overlap. The results we discuss are in the limit when the spring constant of this potential Hl^2/kT is very large, although we will briefly mention what happens if we make these potentials softer. We also describe the knot tracking algorithm in the SI. Briefly, we project the chain onto a plane parallel to the extension axis and determine the smallest subset of crossings that retains the chain topology via computation of the Alexander polynomial, a knot invariant.[6,20,30,31] The resulting statistics of the knotted region (e.g., boundary and midpoint) are measured in terms of the contour coordinate along the chain (i.e., chain index).

Figure 1b shows typical trajectories of a knot's midpoint along the contour of a flexible polymer chain (i.e., $l = 2l_p$) when the bead size is equivalent to the rod length ($b = l$). At low applied tensions f, the knot traverses the chain in a continuous fashion, while at larger tensions the knot jams and makes slow, discrete hops. The dramatic slowdown in the knot's motion is readily apparent in these figures. At force $f = 5\ kT/l$, the knot moves an order of 100 beads in the time of 20 000 rod diffusion times ($l^2\zeta/kT$), while at force $f = 25kT/l$, the knot travels about 20 times a shorter distance in the same time period. We plotted the mean-squared displacements for each of these trajectories and verified that the long-time motion is diffusive (Figure 1c). Interestingly, we also showed that the discrete hopping motion follows Poisson statistics, which we illustrate in the SI.

The above results are for a 3_1 chain topology (Alexander–Briggs notation).[32] How are the transport properties affected by other knot types? In Figure 2a, we plot the knot diffusivity as a function of pulling force f for the case of flexible chains ($l = 2l_p$) and equal bead size to rod length ($b = l$). The diffusivity decreases exponentially beyond a critical force f^*, and this trend appears similar for all the topologies studied thus far—the 3_1, 4_1, 5_1, and 5_2 knots, the ones most common *in vitro*.[33] The dotted line in the figure represents the effective diffusion constant for a particle in a periodic potential. We do not expect this theory to quantitatively capture the knot mobility but rather explain some key trends. When a knot reptates along a polymer with corrugated short-range interactions, the knot experiences an energy landscape that is periodic along the chain contour. We describe the origin of this energy landscape later in the paper, but for now we say that it is $V(x) = 0.5\Delta E \sin(2\pi x/b)$, where ΔE is the activation energy barrier and b is the bead size (the corrugation length). With this assumption, the diffusivity becomes[34,35]

$$D = \frac{D_0}{I_0(z)I_0(-z)}; \quad z = \frac{\Delta E}{2kT} = \frac{fd^*}{2kT} \tag{1}$$

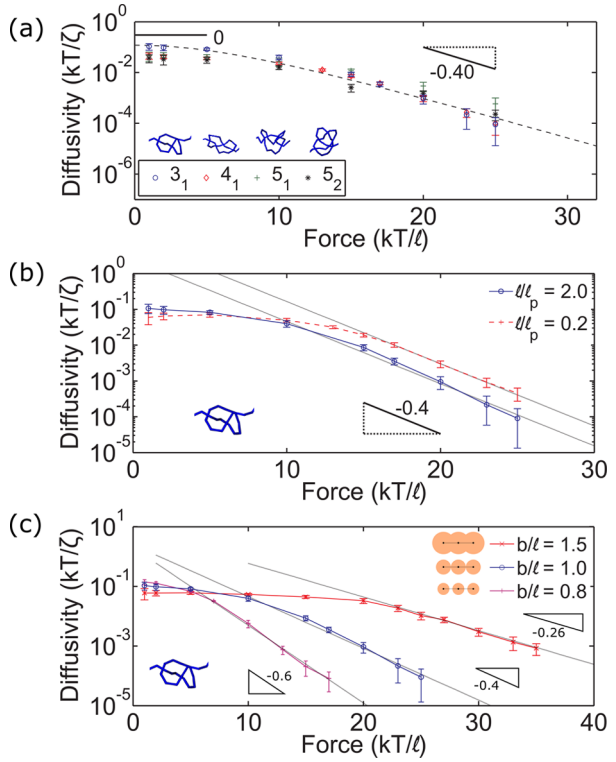

Figure 2. (a) Knot diffusivity vs. applied force for different knot topologies. The chain is flexible ($l = 2l_p$) with bead size equal to the rod length ($b = l$). Dotted line is eq 1 with parameters $D_0 = 0.12$ and $d^* = 0.40$. (b) Knot diffusivity for a 3_1 knot when varying the chain's persistence length. The bead size here is equal to the rod length ($b = l$). (c) Knot diffusivity for a 3_1 knot as a function of bead size. The chain is flexible ($l = 2l_p$) for this graph.

DOI: 10.1021/acsmacrolett.5b00737
ACS Macro Lett. 2016, 5, 123–127

In the above equation, $I_0(z)$ is a modified Bessel function, D_0 the diffusivity at zero force, and d^* the length scale of the activation barrier. At zero force, the expression goes to a constant: $D \to D_0$. When the force is very large, i.e., $fd^*/kT \gg 1$, the diffusivity exhibits Arrhenius scaling, a.k.a. exponential decay, regardless of the form of the potential: $D \to D_0 \exp(-fd^*/kT)$. We see that this expression does a reasonable job capturing the trends observed in the simulation. In actuality, the knot diffusivity is nonmonotonic at low forces as shown by Huang and Makarov.[23] Furthermore, we are unaware of any experimental or theoretical study in the regime $fl_p/kT \ll 1$ where the chain is not extended. This regime is conceptually quite different than what has been examined thus far and would be interesting to inspect in the future.

The key feature of our findings is that the knot diffusivity decays exponentially during jamming, and the rate of decay has a length scale d^* that is comparable to the corrugation of the polymer ($d^* \approx 0.40l$ in Figure 2a). Does this length scale d^* depend on the bending modulus of the polymer chain? In Figure 2b, we plot the diffusivity of a 3_1 knot as a function of force for flexible ($l = 2l_p$) and semiflexible ($l = 0.2l_p$) chains. For both simulations, the bead size is equal to the rod length ($b = l$). We observe that the diffusivity decays exponentially with increasing force, with the decay rate being indistinguishable as long as we scale the force by kT/l, a.k.a., the thermal energy divided by the rod length. Thus, it appears that the bending modulus of the polymer does not affect the decay rate of the knot's diffusivity but instead alters the force f^* at which jamming occurs. In general, stiffer chains require a larger critical tension f^* to overcome the bending penalty for tightening the knot, which leads to a delayed onset of jamming.

Unlike bending, the excluded volume interactions along the chain play a large role in modifying the jamming transition as well as the decay rate of the knot's diffusivity. Figure 2c plots the diffusivity of a 3_1 knot along a flexible chain ($l = 2l_p$) for three different bead sizes: $b = 1.5l$ (overlapping beads), $b = l$ (touching beads), and $b = 0.8l$ (nontouching beads). We find that the critical tension f^* is larger for the overlapping bead case ($b = 1.5l$) compared to the touching bead case ($b = l$). The diffusivity decays more slowly as well. To explain the trend in f^* for these two cases, we note that the excluded volume is corrugated along the polymer contour with a periodicity equal to the rod length l. However, the amplitude is smaller for the overlapping bead case, which results in a lower effective friction between two chain segments when they slide over each other. Thus, the polymer with overlapping beads is less likely to jam at a given tension than the one with touching beads. We can repeat a similar argument for the case when the beads are nontouching ($b = 0.8l$). In this case, segments that slide past each other can get trapped in the crevices between two beads. This trapping leads to arrested motion at lower forces, hence a lower f^*.

We explain the trends in the decay rate of the knot's diffusivity later. For now, let us examine the reptation moves of the knot as it traverses the chain. The results shown below are for the case when the bead size is the same as the rod ($b = l$). At high applied tensions $fl/kT \gg 1$, we find that each reptation event consists of one bead propagating through the knotted core, during which the knot transiently swells by one bead (Figure 3a). Outside of this event, the knot remains jammed with a knot size that is fairly constant in time. In Figure 3b, we see that the time scale of reptation is much smaller than the typical time τ a knot spends in a jammed state. This observation

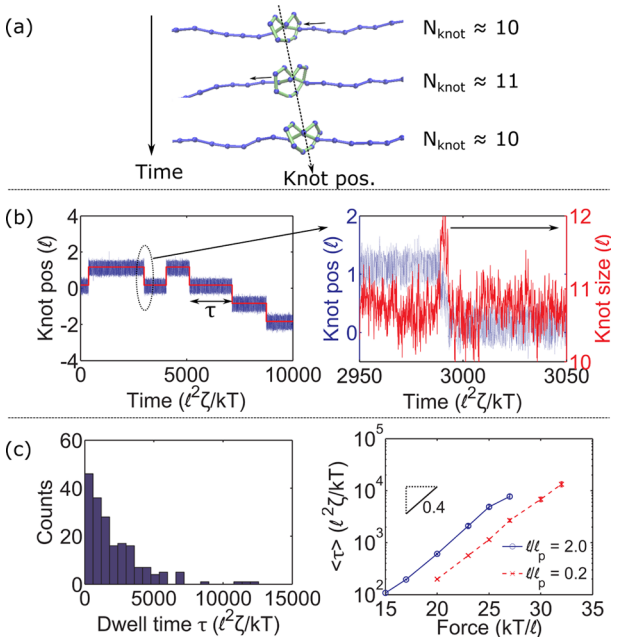

Figure 3. (a) Reptation schematic. The beads are drawn small for illustration purposes. (b) Left: knot position vs. time for a 3_1 knot on a flexible chain ($f = 23kT/l$, $l = 2l_p$). We also plot a piecewise constant fit to the trajectory. Right: if we zoom into a hop, we see that the knot size swells by one bead during reptation. (c) Left: dwell time distribution of knot position for a 3_1 knot. $f = 23kT/l$, $l = 2l_p$. Right: Average dwell time vs. applied force for a 3_1 knot. The slope gives the length scale of the activation barrier for reptation. We plot for both flexible ($l = 2l_p$) and semiflexible ($l = 0.2l_p$) chains. For all plots shown here, the bead size is equivalent to the rod length ($b = l$).

indicates that the first step of reptation—i.e., the process by which a bead enters the knotted core—is the rate-limiting step for the knot's motion. If we fit the knot's trajectory to a piecewise constant function[36] (binning over a time larger than the reptation time of a knot), we can extract a dwell time distribution for the knot position as shown in Figure 3c. Using Kramers theory of activated processes,[37] the average caging time of the knot follows the scaling

$$\langle \tau \rangle \sim \exp(\Delta E/kT) \tag{2}$$

where ΔE is the activation barrier for the first step of reptation ($\Delta E/kT \gg 1$). Thus, if we plot the average caging time versus applied force on a log scale, we determine how the activation barrier scales with this parameter (Figure 3c). We find that the activation energy scales linearly with force at large forces: $\Delta E \sim fd^{**}$, $fl/kT \gg 1$. Furthermore, we find that the length scale of this barrier matches to the length scale for the decay of diffusivity mentioned earlier: $d^{**} \approx d^*$. This suggests that the first step of reptation is the dominant contribution to the energy landscape of the knot's motion.

This result may explain why the knot diffusivities appear to be relatively insensitive to chain topology, at least for the simple knot types examined thus far (3_1, 4_1, 5_1, and 5_2) (Figure 2a). The first reptation move is similar for these knot types, and hence the scaling for diffusivity vs. force should be similar as well. Of course, we expect this universality will break down for knots with an extremely large number of crossings, where the energy landscape will be much more complex. In this situation, the first step in reptation will no longer be rate-limiting, and the

DOI: 10.1021/acsmacrolett.5b00737
ACS Macro Lett. 2016, 5, 123−127

knot's dynamics will be dominated by the details of how the contour snakes through the interior of the knot.

In the above point, we note that the energy landscape of the knot may change considerably if the knot spends a significant amount of time in the swollen phase during reptation—in other words, the propagation of chain through the knotted core is sluggish. A natural question to ask then is if the softness of the excluded volume interactions alters this effect. We examine this idea in the SI. We find that by making the harmonic potential between the beads become softer we can lengthen the time the knot spends in reptation. Since very little is known about this field, a more systematic study of the effects of chain softness merits examination for the future.

In the last part of this paper, we provide an argument to explain the relative trends on how the excluded volume alters the decay rate in the knot diffusivity. Our argument involves estimating the relative activation energy barriers for the reptation process. In Figure 4a, we show snapshots of a highly

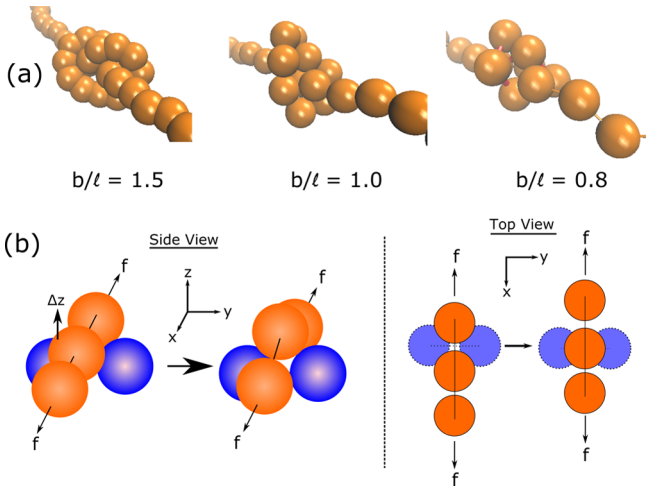

Figure 4. (a) Snapshots of a 3_1 knot with different bead sizes. (b) A tensed, bead−rod chain sliding over another chain. We compute the displacement Δz the top chain must make in order to move over the second chain via bending.

tensed, 3_1 knot with three different bead sizes: $b = 1.5l$ (overlapping beads), $b = 1.0l$ (touching beads), and $b = 0.8l$ (nontouching beads). To a first approximation, the activation barrier for a bead entering the knotted region scales as $\Delta E \sim N_{\mathrm{ring}}\Delta E_{\mathrm{slide}}$, where $\Delta E_{\mathrm{slide}}$ is the energy barrier for two segments to slide past each other, and N_{ring} is the number of segment pairs that participate in this motion, which is roughly equal to the ring size of the knotted entrance ($N_{\mathrm{ring}} \approx 4$ for $b = 0.8l$, 6 for $b = 1.0l$, and 9 for $b = 1.5l$). To get an estimate for $\Delta E_{\mathrm{slide}}$, we examine the motion of a bead−rod chain under a uniform tension f sliding over another fixed chain (Figure 4b). The top chain initially rests between the crevices of the bottom chain, and we determine how much the top chain must bend for its middle to lie completely above the lower chain. In the limit of large tension ($fl/kT \gg 1$) and small vertical displacements ($\Delta z/l \ll 1$), the energy penalty for this motion scales as $\Delta E_{\mathrm{slide}} \sim f\Delta z^2/l$, where l is the rod length. We calculated Δz^2 for the three different bead sizes in the SI, which yields $\Delta z^2 = 0.0627l^2$ for $b = 0.8l$, $0.0252l^2$ for $b = l$, and $0.0083l^2$ for $b = 1.5l$. Notice that the rougher the polymer surface, the larger the displacement Δz needed for sliding to occur. Combining all these results gives the total activation barrier $\Delta E \sim N_{\mathrm{ring}}\Delta z^2 f/l$. Taking the ratio of the barriers for the three cases listed above, we obtain $\Delta E[b = 1.5l]/\Delta E[b = l] = 0.49$ and $\Delta E[b = 0.8l]/\Delta E[b = l] = 1.7$, which compares reasonably to the relative decay rates $r^* = -d(\log D)/df$ of the knot diffusivities: $r^*[b = 1.5l]/r^*[b = l] = 0.65$ and $r^*[b = 0.8l]/r^*[b = l] = 1.5$ (see Figure 2c). Of course, these crude estimates neglect several effects such as how the chain connectivity in the knotted entrance alters the sliding energy $\Delta E_{\mathrm{slide}}$. We do not expect quantitative agreement but rather hope that this analysis provides insight into the factors that contribute to the reptation activation barrier.

In this study, we examined the motion of a knot along a tensioned chain, surveying the role that bending, knot topology and excluded volume plays in this process. The knot dynamically arrests above a critical tension, beyond which the knot's diffusivity decays exponentially. We note that the physics described here is analogous to the glassy dynamics in colloidal systems,[38,39] where particles get "caged" at short times but escape this cage by rearranging its microstructure.[40] It would be fascinating to study the relaxation of a jammed knot to see if glassy effects such as aging occur in these systems. Similarly, it would be interesting to explore the effects of chain attraction on jamming, as it has been shown that attractive potentials alter the physics of the glass transition considerably.[39,41] We note that this work gives insight into how friction between entanglements is modified by a corrugated energy landscape along the polymer backbone. This idea could be important in developing more accurate entanglement models or augment existing theories such as the "tube" models from Edwards and DeGennes.[42,43] This work may also be amenable to study macroscopic, granular chains, where there has been recent interest in understanding knotting effects.[44,45] Lastly, after initial submission of this work, Micheletti and co-workers quantified how the topology of knots alters their mobility when jamming at a nanopore.[27] We note that in this high force regime friction is highly nonlinear and thus sensitive to the configuration of the chain. It is likely that chain asymmetries from the nanopore could give rise to different trends in the knot mobility as a function of chain topology. This topic would be interesting to examine in the future.

■ ASSOCIATED CONTENT

Supporting Information

The Supporting Information is available free of charge on the ACS Publications website at DOI: 10.1021/acsmacrolett.5b00737.

Simulation details, sensitivity to total chain length, Poisson statistics of knot hopping, effect of soft excluded volume interactions, and details of sliding friction model (PDF)

■ AUTHOR INFORMATION

Corresponding Author

*E-mail: pdoyle@mit.edu.

Present Address

†Liquiglide, 75 Sidney Street, Cambridge, MA 02139, USA.

Author Contributions

‡These authors contributed equally

Notes

The authors declare no competing financial interest.

DOI: 10.1021/acsmacrolett.5b00737
ACS Macro Lett. 2016, 5, 123−127

■ ACKNOWLEDGMENTS

This work is supported by the Singapore-MIT Alliance for Research and Technology (SMART) and National Science Foundation (NSF) grant CBET-1335938.

■ REFERENCES

(1) Liu, L. F.; Perkocha, L.; Calendar, R.; Wang, J. C. *Proc. Natl. Acad. Sci. U. S. A.* **1981**, *78*, 5498−5502.
(2) Wasserman, S. A.; Cozzarelli, N. R. *Science* **1986**, *232*, 951−960.
(3) Wang, J. C. *J. Mol. Biol.* **1971**, *55*.
(4) Meluzzi, D.; Smith, D. E.; Arya, G. *Annu. Rev. Biophys.* **2010**, *39*, 349−366.
(5) Adams, C. C. *The Knot Book: An Elementary Introduction to the Mathematical Theory of Knots*; American Mathematical Society, 2004.
(6) Vologodskii, A. Monte Carlo Simulation of DNA Topological Properties. *Topology in Molecular Biology*; Springer, 2007.
(7) Bao, X. R.; Lee, H. J.; Quake, S. R. *Phys. Rev. Lett.* **2003**, *91*, 265506.
(8) Arai, Y.; Yasuda, R.; Akashi, K.; Harada, Y.; Miyata, H.; Kinosita, K.; Itoh, H. *Nature* **1999**, *399*, 446−448.
(9) Ayme, J. F.; Beves, J. E.; Leigh, D. A.; McBurney, R. T.; Rissanen, K.; Schultz, D. *Nat. Chem.* **2011**, *4*, 15.
(10) Tang, J.; Du, N.; Doyle, P. S. *Proc. Natl. Acad. Sci. U. S. A.* **2011**, *108*, 16153−16158.
(11) Renner, C. B.; Du, N.; Doyle, P. S. *Biomicrofluidics* **2014**, *8*, 034103.
(12) Renner, C. B.; Doyle, P. S. *Soft Matter* **2015**, *11*, 3105−3114.
(13) Sumners, D.-W.; Whittington, S. G. *J. Phys. A: Math. Gen.* **1988**, *21*, 1689.
(14) Janse van Rensburg, E. J.; Sumners, D. A. W.; Wasserman, E.; Whittington, S. G. *J. Phys. A: Math. Gen.* **1992**, *25*, 6557−6566.
(15) Taylor, W. R. *Nature* **2000**, *406*, 916−919.
(16) Lua, R. C.; Grosberg, A. Y. *PLoS Comput. Biol.* **2006**, *2*, e45.
(17) Virnau, P.; Mirny, L. A.; Kardar, M. *PLoS Comput. Biol.* **2006**, *2*, e122.
(18) Kivotides, D.; Wilkin, S. L.; Theofanous, T. G. *Phys. Rev. E* **2009**, *80*, 041808.
(19) Di Stefano, M.; Tubiana, L.; Di Ventra, M.; Micheletti, C. *Soft Matter* **2014**, *10*, 6491−6498.
(20) Renner, C. B.; Doyle, P. S. *ACS Macro Lett.* **2014**, *3*, 963−967.
(21) Matthews, R.; Louis, A.; Yeomans, J. M. *EPL-Europhys. Lett.* **2010**, *89*, 20001.
(22) Vologodskii, A. *Biophys. J.* **2006**, *90*, 1594−1597.
(23) Huang, L.; Makarov, D. E. *J. Phys. Chem. A* **2007**, *111*, 10338−10344.
(24) Rosa, A.; Di Ventra, M.; Micheletti, C. *Phys. Rev. Lett.* **2012**, *109*, 118301.
(25) Huang, L.; Makarov, D. E. *J. Chem. Phys.* **2008**, *129*, 121107.
(26) Szymczak, P. *Biochem. Soc. Trans.* **2013**, *41*, 620.
(27) Suma, A.; Rosa, A.; Micheletti, C. *ACS Macro Lett.* **2015**, *4*, 1420−1424.
(28) Kirmizialtin, K.; Makarov, D. E. *J. Chem. Phys.* **2008**, *128*, 094901.
(29) Ward, A.; Hilitski, F.; Schwenger, W.; Welch, D.; Lau, A. W. C.; Vitelli, V.; Mahadevan, L.; Dogic, Z. *Nat. Mater.* **2015**, *14*, 583−588.
(30) Dai, L.; Renner, C. B.; Doyle, P. S. *Macromolecules* **2014**, *47*, 6135−6140.
(31) Vologodskii, A. *Monte Carlo Simulation of DNA Topological Properties. Topology in Molecular Biology* **2007**, 23.
(32) Rolfsen, D. *Table of Knots and Links, Appendix C* **1976**.
(33) Rybenkov, V. V.; Cozzarell, N. R.; Vologodskii, A. V. *Proc. Natl. Acad. Sci. U. S. A.* **1993**, *90*, 5307.
(34) Zwanzig, R. *Proc. Natl. Acad. Sci. U. S. A.* **1988**, *85*, 2029−2030.
(35) Ma, X.; Lai, P.-Y.; Ackerson, B. J.; Tong, P. *Phys. Rev. E* **2015**, *91*, 042306.
(36) Little, M. A.; Jones, N. S. *Proc. R. Soc. London, Ser. A* **2011**, *467*, 3115−3140.
(37) Kramers, H. A. *Physica (Amsterdam)* **1940**, *7*, 284.
(38) Hunter, G. L.; Weeks, E. R. *Rep. Prog. Phys.* **2012**, *75*, 066501.
(39) Sciortino, F.; Tartaglia, P. *Adv. Phys.* **2005**, *54*, 471−524.
(40) Schweizer, K. S.; Yatsenko, G. *J. Chem. Phys.* **2007**, *127*, 164505.
(41) Dawson, K. A. *Curr. Opin. Colloid Interface Sci.* **2002**, *7*, 218−227.
(42) de Gennes, P. G. *J. Chem. Phys.* **1971**, *55*, 572.
(43) Edwards, S. F. *Proc. Phys. Soc., London* **1967**, *91*, 513.
(44) Belmonte, A.; Shelley, M. J.; Eldakar, S. T.; Wiggins, C. H. *Phys. Rev. Lett.* **2001**, *87*, 114301.
(45) Ben-Naim, E.; Daya, Z. A.; Vorobieff, P.; Ecke, R. E. *Phys. Rev. Lett.* **2001**, *86*, 1414.

DOI: 10.1021/acsmacrolett.5b00737
ACS Macro Lett. 2016, 5, 123−127